Preprints of the 21st IFAC World Congress (Virtual)
Berlin, Germany, July 12-17, 2020

Trajectory Planning and Vehicle Control at low speed for home zone manoeuvres

G. Borrello*, E. Raffone*, C. Rei*, M. Fossanetti*

** Advanced E/E - DAS – Control Systems*
Centro Ricerche FIAT S.c.p.A.
Strada Torino 50, 10043 Orbassano (Turin – Italy)
(Tel: +39 011 9080334; e-mail: enrico.raffone@crf.it)

Abstract: Trajectory Planning and Vehicle Control at low speed is the automation of traditional manual vehicle maneuvers in home zones. We refer to living streets that are designed primarily to meet the needs of pedestrians, cyclists, children and residents and where the speeds and dominance of the cars are limited. In this study, we present the trajectory planning and vehicle control by using model predictive control (MPC) both for lateral and longitudinal dynamics. In particular, the lateral control of the vehicle solves a convex optimization with steering and lateral travel range constraints. It is based on a linear model of vehicle kinematics which is synthesized from nonlinear dynamics by using time-state control form (TSCF) transformation. The longitudinal model predictive control is based on a simple double integrator model with longitudinal travel and speed references. The performance of the proposed method is verified with a V-cycle model-based approach, starting from Model-in-the-Loop simulation through vehicle experiments on Jeep Renegade prototypal vehicle.

Keywords: Autonomous Vehicles; Trajectory and Path Planning; Motion control.

1. INTRODUCTION

In the last years, new cars have changed. What was mainly mechanical transportation means has now been fully packed with advanced technology. The evolution started slowly at the beginning, while it is much faster now. What was thought as a way to avoid collisions at relatively low speed has evolved so far. For example, the newest cars can now avoid collisions with many types of obstacles by steering as well as braking. Nowadays, tools assist the everyday driving by keeping the car inside the lanes and controlling the relative speed to other road-users. Self-driving cars are going to loom on the horizon.

Before humans take their hands off the steering wheel completely, there will be an increasing level of advanced driver assistance systems (ADAS). This will help the driver avoid accidents due to human error saving both lives and money. Although higher speed results in more severe accidents, more than 50,000 crashes occur in parking lots annually in the US, resulting in 500 or more deaths and more than 60,000 injuries according to the National Safety Council (see *US NSC Parking lot safety (2019)*). Furthermore, the Swedish Road Insurance Association estimated a cost of parking-related accidents in Sweden equal to 229 MLN SEK (21 MLN EUR) in 2015, with an increasing trend in last years (*Trafikförsäkringsföreningen - årsredovisning 2015*).

Literature demonstrate the importance and the significance of working on automated manoeuvres at low speed. Our activity about has considered to use a theoretical approach that solve the problem of vehicle control and trajectory planning at low speed in a general way, such that the vehicle could face different scenarios by minimizing the specific code for.

In the next paragraphs, the paper is structured as follows: Section 2 presents the prototypal vehicle setup for control development. The design model is included in Section 3, whereas Section 4 includes control problem explanation and solution design. Section 5 reports the experimental validation and simulation on the same test track are presented, near to FCA Research and Development Technical Center. Some conclusions are drawn in Section 6.

Fig. 1. *Jeep Renegade prototypal vehicle.*

2. PROTOTYPAL VEHICLE SETUP FOR CONTROL DEVELOPMENT

2.1 Vehicle

The prototypal vehicles which has been used during the development is a Jeep Renegade 1.6 Multijet with dual dry clutch transmission (DDCT).

2.2 Sensors platform

The main sensors that equip the vehicle are traditional normal production Electronic Stability Control (ESC) inertial Active Chassis sensors: longitudinal/lateral acceleration and yaw rate sensors (*Konrad (2015)*). Then, as fundamental sensor that links vehicle signals to surroundings references which has been used is Novatel dual antenna Global Navigation Satellite System (GNSS), two Manta forward-looking stereo camera sensors, six Ibeo LIDAR, normal production forward-looking camera, radar, and twelve Ultra Sound Scan sensors. In our paper and related development, the main sensors involved are traditional ESC sensors plus GNSS positioning system.

2.3 Actuators: steering, braking and powertrain

Electric Power Steering (EPS) uses an electric motor to assist the driver of a vehicle. Sensors detect the position and torque of the steering column and an ECU applies assistive torque via the motor, which connects to either the steering gear or steering column. This allows varying amounts of assistance to be applied depending on driving conditions. Jeep Renegade is equipped with a TRW/ZF column EPS, able to be driven by using traditional ParkAssist HWTO (HandWheel Torque Overlay) interface on vehicle C-CAN network. In particular, the normal production HWTO interface has been modified in terms of maximum vehicle speed, in order to use the EPS as a mechatronic unit able to steer the vehicle, and not to only assist the driver anymore.

Braking system module (BSM) provides the functional interface to realize an acceleration/deceleration action of the vehicle. In detail, in our prototypal vehicle, we used a SW modified TRW/ZF EBC 460. This ECU provides on vehicle C-CAN network a functional channel able to be a gateway of acceleration / positive torque to the powertrain ECU (ECM) and the way to decelerate the vehicle by brakes. The normal production parking longitudinal interface has been modified in order to achieve technical targets of present work. Also the DDCT ECU SW has been modified in order to manage the longitudinal manoeuvres from/to 0/15 km/h around to 0 Nm of engine torque in a comfortable way.

3. VEHICLE MODEL

Next, we introduce the vehicle models used for Trajectory Planning and Control. The well-known dynamic models are undefined or ill-conditioned at low speeds. As shown to be effective in *Polack et al. (2017)* and *Kong et al. (2015)*, the model used for low speed application (0÷20 km/h) is the kinematic bicycle model.

3.1 Lateral vehicle model

The 4 d.o.F. kinematic bicycle model is one of the simplest models used in motion planning. In this model, the two left and right front wheels are represented by one single wheel at point A (see fig.2). Similarly, the rear wheels are represented by one central rear wheel at point B.

The steering angles for the front and rear wheels are represented by δ_f and δ_r respectively.

The model is derived assuming that only the front wheel can be steered (δ_r =0). For that reason and simplicity, we will use the notation $\delta = \delta_f$.

The resulting kinematic bicycle model (fig. 2) is described by the following state-space equations in the Inertial frame:

$$\dot{x} = v\,cos(\psi) \tag{1}$$

$$\dot{y} = v\,sin(\psi) \tag{2}$$

$$\dot{\psi} = \frac{v}{L} tan\,\delta \tag{3}$$

$$\dot{v} = a \tag{4}$$

In particular *x,y* are the Cartesian coordinates of the vehicle's rear wheel, while ψ describes the orientation (Yaw angle) of the vehicle. *v* and *a* denote the velocity and longitudinal acceleration respectively. Thus, the state and input vectors of this model can be defined as $\boldsymbol{X}=[x,y,\psi,v]$ and $\boldsymbol{U}=[\delta,a]$, respectively.

Since the kinematic model described is nonlinear, we utilize the Time-State Control Form (TSCF) (*Kiyota H. et al. (1998)*), as described by *Oyama K. et al. (2013)*. Thanks to this approach, the lateral dynamic is linearized and represented as a differential equation w.r.t. the state (x) instead of time.

Dividing (2) and (3) by (1), we get the following TSCF:

$$\begin{aligned} \frac{dy}{dx} &= tan(\psi) \\ \frac{d\psi}{dx} &= \frac{tan(\delta)}{L\,cos(\psi)} \end{aligned} \tag{5}$$

Let's also introduce the nonlinear state and input transformation:

$$\begin{bmatrix} z_1 \\ z_2 \\ z_3 \end{bmatrix} = \begin{bmatrix} x \\ y \\ dy/dx \end{bmatrix} = \begin{bmatrix} x \\ y \\ tan(\psi) \end{bmatrix} \tag{6}$$

$$\mu_1 = v\,cos(\psi) \tag{7}$$

$$\mu_2 = \frac{tan(\delta)}{L\,cos^3(\psi)} \tag{8}$$

By applying the transformation to (5) we obtain two linear subsystems given by:

$$\frac{dz_1}{dt} = \mu_1 \tag{9}$$

$$\frac{dt}{dz_1}\begin{bmatrix} \frac{dz_2}{dt} \\ \frac{dz_3}{dt} \end{bmatrix} = \begin{bmatrix} 0 & 1 \\ 0 & 0 \end{bmatrix}\begin{bmatrix} z_2 \\ z_3 \end{bmatrix} + \begin{bmatrix} 0 \\ 1 \end{bmatrix}\mu_2 \tag{10}$$

In which the first one is a differential equation w.r.t. time, the second depends on the time-state *x*. The actual steering angle δ is computed using μ_2 and ψ by inverting (8):

$$\delta = tan^{-1}(L\,cos^3(\psi)\mu_2) \tag{11}$$

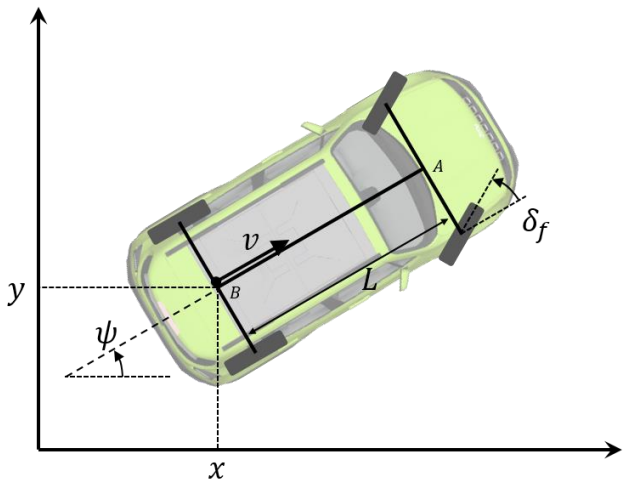

Fig. 2. *Inertial and Vehicle reference frames for lateral control.*

3.2 Longitudinal vehicle model

In general, the point-mass model is not used for design lateral controllers due to their large modelling errors. However, those models are widely used for longitudinal control purposes. In this work, the vehicle's longitudinal motion is described, in the Vehicle frame, as a double integrator system, in which the states are the travelled distance (ξ) and the vehicle speed (v):

$$\dot{\xi} = v \tag{12}$$

$$\dot{v} = a \tag{13}$$

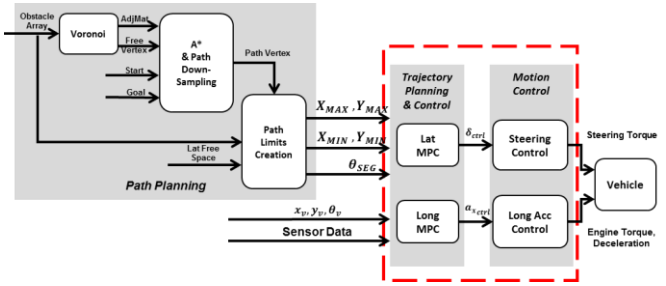

Fig. 3. *General block diagram, in dotted red box main contents included in presented work.*

4. CONTROL DESIGN

Fig. 3 shows the general block diagram for low speed manoeuvres planning and automated control. In particular, the general idea foresees starting from a map of static obstacles in order to build a path (path planning block). From a defined path that we can consider as the half of free space, it passes to the '*trajectory planning & control*' and '*motion control*' blocks that are the targets of this paper. The inputs for trajectory planning at low speed are the points of calculated path and sensors information about dynamic obstacles in the scenario. The next paragraphs of Control Design are going to be presented how lateral and longitudinal vehicle trajectory is planned, considering the following as inputs: the desired path and dynamic obstacles, these represented as space constraints in the vehicle reference frame.

4.1 Trajectory Planning and Control

Model Predictive Control (MPC) has been developed considerably over the last two decades. The main advantage of MPC is the fact that it allows the current timeslot to be optimized while taking future time-slots in account. This is achieved by optimizing a finite time-horizon, but only implementing the first time-slot.

MPC can manage future profiles of reference and constraints and anticipate control actions accordingly with them. These limits may be imposed on any part of the system variables, such as states, outputs, inputs, and considering main actuators characteristics and operative limitations.

4.1.1 Lateral MPC

From (10), to control z_2 and z_3 using μ_2, the MPC controls the lateral vehicle dynamics to track the optimal path according to constraints on the steering limitation and free space corridor. Discretizing (10) by using Tustin method, we obtain:

$$\begin{bmatrix} z_2(k+1) \\ z_3(k+1) \end{bmatrix} = \begin{bmatrix} 1 & \Delta_s \\ 0 & 1 \end{bmatrix} \begin{bmatrix} z_2(k) \\ z_3(k) \end{bmatrix} + \begin{bmatrix} \Delta_s^2/2 \\ \Delta_s \end{bmatrix} \mu_2(k) \tag{14}$$

Where Δ_s is the step w.r.t. the time-state x (positive or negative respectively for forward or backward motion): in other words, Δ_s is not a time step, but it's the delta distance of movement along x. Denoting the state vector, $z = [\ z_2\ \ z_3\ ]^T$, the control horizon, H, the weight diagonal positive definite matrices Q and R, the general performance index for path tracking control is defined as:

$$J = \boldsymbol{z}(H)^T Q_{fin}\, \boldsymbol{z}(H) + \sum_{k=0}^{H-1} \boldsymbol{z}(k)^T Q\, \boldsymbol{z}(k) + R\mu_2(k)^2 \tag{15}$$

Subject to the constraints:

$$z_{2_{min}}\ (z_1) \le z_2 \le\ z_{2_{max}}\ (z_1) \tag{16}$$

$$\delta_{min} \le \delta \le \delta_{max} \tag{17}$$

Let's consider from the (11) the function:

$$\Gamma\ (z_3, \mu_2) = l\, cos^3(tan^{-1}(z_3))\mu_2 \tag{18}$$

Thanks to which it is possible to rewrite (18) as:

$$tan(\delta_{min}) \le \Gamma(z_3, \mu_2) \le tan(\delta_{max}) \tag{19}$$

Since it is a nonlinear function of z_3, in order to solve the optimization through linear constraints, it is approximated with a first-order Taylor series expansion:

$$\hat{\Gamma}(z_3, \mu_2) = \Gamma\big(\hat{z}_3(k), \hat{\mu}_2(k)\big) + \frac{d\Gamma}{dz_3}\big(z_3 - \hat{z}_3(k)\big) + \frac{d\Gamma}{d\mu_2}\big(\mu_2 - \hat{\mu}_2(k)\big) \tag{20}$$

With:

$$\frac{d\Gamma}{dz_3} = -\frac{sin(tan^{-1}(z_3))3L\,cos^3(tan^{-1}(z_3))\,\mu_2}{1+\hat{z}_3{}^2(k)} \quad (21)$$

$$\frac{d\Gamma}{d\mu_2} = l\,cos^3(tan^{-1}(z_3)) \quad (22)$$

Where $\hat{\mu}_2(k)$ is the input of previous sampling and $\hat{z}_3(k)$ is the predicted state using the input of previous sampling and initial current state. Hence, the constraint related to the steering angle is approximated by:

$$tan(\delta_{min}) \le \hat{\Gamma}(z_3,\mu_2) \le tan(\delta_{max}) \quad (23)$$

Thus, we can rewrite the lateral MPC formulation as:

$$\begin{aligned}&\boldsymbol{J}(z_2,z_3)\\&=\begin{bmatrix}y_{ref}(H_{lat})-z_2(H_{lat})\\-z_3(H_{lat})\end{bmatrix}^T\boldsymbol{Q_f}\begin{bmatrix}y_{ref}(H_{lat})-z_2(H_{lat})\\-z_3(H_{lat})\end{bmatrix}\\&+\sum_{k=1}^{H_{lat}-1}\begin{bmatrix}y_{ref}(k)-z_2(k)\\-z_3(k)\end{bmatrix}^T\boldsymbol{Q}\begin{bmatrix}y_{ref}(k)-z_2(k)\\-z_3(k)\end{bmatrix}\\&+\sum_{k=0}^{H_{lat}-1}\boldsymbol{R}\,\mu_2^2(k)\end{aligned} \quad (24)$$

Subject to:

$$\boldsymbol{Y_{MIN}} \le \boldsymbol{z_2}(k) \le \boldsymbol{Y_{MAX}} \quad (25)$$

$$\begin{aligned}&tan(\delta_{min}) \le\\&\hat{\Gamma}(z_3,\mu_2)+\frac{d\Gamma}{dz_3}\left(z_3-\hat{z}_3(k)\right)+\frac{d\Gamma}{d\mu_2}\left(\mu_2-\hat{\mu}_2(k)\right)\\&\le tan(\delta_{max})\end{aligned} \quad (26)$$

The main problems of this approach are the representation singularities introduced by the model, defined for-π/2<ψ<π/2, and the error introduced by the linearization.

The innovative contribution in our solution is that the developed algorithm smoothly rotates the path in the vehicle system in order to manage cases in which the vehicle has to follow a path with bends greater than π/2. The aim is to avoid singularities, to reduce the linearization errors at each time step, and to maximize the length of the section of path usable by MPC. In this way, we obtain maximum flexibility of scenario coverage.

In detail, once the path is defined as a set of segments, the algorithm, at each step time, firstly defines in which segment the vehicle is located. Then, by using the orientation angles of the actual segment (θ_i), and the next one (θ_{i+1}), the path is dynamically rotated using a linear interpolation and a weighted (W) "corrective factor" which considers also θ_{i+2} through (27), where (x_v,y_v) are the current vehicle's coordinates, d is the Euclidean distance between the vehicle and the end point of the actual segment (x_i,y_i) and $d_{i+1,i}$ is the distance between the current and the next segment.

$$\theta_{ROT} = W\frac{(\theta_{i+2}-\theta_{i+1})d}{d_{i+1,i}} + \frac{(\theta_{i+1}-\theta_i)d}{d_{i+1,i}} + \theta_i \quad (26)$$

4.1.2 Longitudinal MPC

Also in this case, the chosen control technique is the linear MPC. This allows us to manage both speed reference and obstacle tracking in a single integrated approach.

To implement a control by using the vehicle's longitudinal motion model, we can firstly discretize the aforementioned system (12, 13):

$$\begin{bmatrix}\xi(k+1)\\v(k+1)\end{bmatrix} = \begin{bmatrix}1 & \Delta_t\\0 & 1\end{bmatrix}\begin{bmatrix}\xi(k)\\v(k)\end{bmatrix} + \begin{bmatrix}\Delta_t^2/2\\\Delta_t\end{bmatrix}a(k) \quad (28)$$

where Δ_t is the time step.

This type of formulation, easily handles problems such as tracking of speed reference and maintenance of position constraints. However, this approach can't handle stationary error due to exogenous disturbances and/or motion control inaccuracy.

To solve this problem, it was decided to add a position reference computed as the difference between the integral of speed reference and Ds_{meas}, which is the travelled space measured from longitudinal control enabled by the wheel speed sensors:

$$\xi_{ref} = \int V_{ref}\,dt - Ds_{meas} \quad (29)$$

The performance index for speed tracking control can be written as:

$$\begin{aligned}&\boldsymbol{J}(\xi,v)\\&=\begin{bmatrix}\xi_{ref}(H_{lon})-\xi(H_{lon})\\V_{ref}(H_{lon})-v(H_{lon})\end{bmatrix}^{\boldsymbol{T}}\boldsymbol{Q_f}\begin{bmatrix}\xi_{ref}(H_{lon})-\xi(H_{lon})\\V_{ref}(H_{lon})-v(H_{lon})\end{bmatrix}\\&+\sum_{k=1}^{H_{lon}-1}\begin{bmatrix}\xi_{ref}(k)-\xi(k)\\V_{ref}(k)-v(k)\end{bmatrix}^{\boldsymbol{T}}\boldsymbol{Q}\begin{bmatrix}\xi_{ref}(k)-\xi(k)\\V_{ref}(k)-v(k)\end{bmatrix}\\&+\sum_{k=0}^{H_{lon}-1}\boldsymbol{R}\,a^2(k)\end{aligned} \quad (30)$$

Subject to the constraints on the position, speed, acceleration and jerk:

$$\boldsymbol{\xi_{MIN}} \le \xi(k) \le \boldsymbol{\xi_{MAX}} \quad (31)$$

$$\boldsymbol{v_{MIN}} \le v(k) \le \boldsymbol{v_{MAX}} \quad (32)$$

$$\boldsymbol{a_{MIN}} \le a(k) \le \boldsymbol{a_{MAX}} \quad (33)$$

$$\frac{\partial}{\partial t}\,\boldsymbol{a_{MIN}}\,\Delta_t \le a(k)-a(k-1) \le \frac{\partial}{\partial t}\boldsymbol{a_{MAX}}\,\Delta_t \quad (34)$$

The general idea regarding speed reference is the following:

- to try to follow the maximum speed allowed along the straight sections and
- to reduce it taking into account:
  - the curvature, ρ, predicted by the lateral MPC, and
  - the maximum allowed lateral acceleration, a_{ymax}:

$$V_{ref} = \sqrt{\frac{a_{y_{max}}}{\rho}} \tag{35}$$

Where the curvature is computed:

$$\rho = \frac{2sin\left(\frac{\theta_i - \theta_{i+1}}{2}\right)}{\frac{\Delta s_i}{cos\left(\frac{\theta_i + \theta_{i+1}}{2}\right)}} \tag{36}$$

4.2 Motion Control

The vehicle models presented in the previous sections assume that the inputs, desired steering wheel angle δ and longitudinal acceleration a, can be directly controlled. However, low level controllers are needed to transform this control input into physical signals for the actuators. In detail, the steering angle control is realized by using the Electronic Power Steering (EPS) system torque interface available on the vehicle CAN network. Similarly, the vehicle longitudinal motion is controlled by means of acceleration/deceleration request to the braking system through normal production (NP) Adaptive Cruise Control interface.

4.2.1 Steering Control

The EPS low level control loop has been designed by using a state feedback controller. This consists of:

1. A linear time invariant Kalman observer that filters/estimates the system states, also useful to estimate driver hands on the steering wheel.

2. An optimal linear quadratic integral controller able to track the steering wheel angle reference from MPC lateral control.

For further details please refer to *Raffone (2016)*, where you can find model based development and related practical considerations.

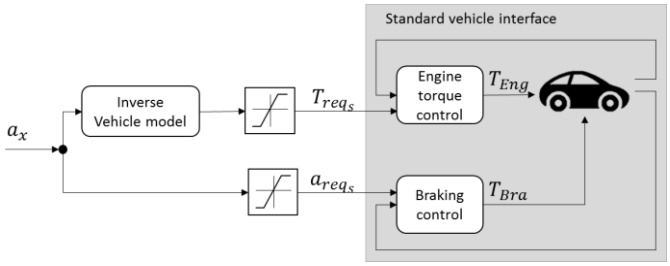

Fig. 4. *General block diagram for longitudinal control setup.*

4.2.1 Longitudinal acceleration control

Conversely to the steering control, the longitudinal acceleration control is managed by multiple actuations (e.g. engine, electric motor, gear-box and braking), hence the interfaces can change according to vehicle architecture, actuator controls and their integration.

In this case, we face a vehicle in which the vehicle interfaces, for longitudinal dynamic control, are:

1. Engine-torque request:delivered to Engine Control (T_{reqs})
2. Deceleration request: delivered to Brake System (a_{reqs})

Aiming to keep the control architecture simply and easy to tune, no further feedback control loop have been introduced at this level. Therefore, implementation of the longitudinal acceleration control, assume the structure shown in fig. 4.

The command a_x is split in two channels, one for each interface. The braking system includes a deceleration closed loop that allows to accept directly deceleration command (a_{reqs}) and to generate a braking torque T_{bra}. The engine control performs a closed-loop control based on an estimation of applied engine torque T_{Eng}. To match the available interface an inverse vehicle model has been implemented in order to convert a_x in T_{reqs}, which considers the current vehicle configuration (e.g. gear ratio, inertia, friction) and mainly exogenous input (e.g. road slope, drag forces). The relative equation can be written as:

$$T_{req} = m(a_x + g\,sin(\alpha))R_w\tau_{gr}\eta_{gr}\tau_{ar}\eta_{ar} + (F_0 + v_xF_1 + v_x^2F_2) \tag{37}$$

Where m is the equivalent vehicle mass, g the gravity acceleration, α the road slope, R_w the loaded wheel radius, τ_{gr} and τ_{ar} are respectively the gearbox and axle ratios, η_{gr} and η_{ar} are the mechanical efficiency of gearbox and transmission and F_0, F_1, F_2 are the coast down coefficients.

5. SIMULATION AND EXPERIMENTAL RESULTS

The proposed algorithm has been first validated via simulation by using IPG CarMaker in a Matlab/Simulink environment. Afterwards, only part of simulation scenarios has been evaluated on Jeep Renegade equipped with a dSPACE MicroAutobox II. The optimization problem solvers were generated by CVXGEN Code Generation for Convex Optimization (*Mattingley et al. (2012)*) for real time execution.

To test the performance of our solution, a series of low speed manoeuvres have been simulated and experimentally tested. The aim is to follow this manoeuvres as close as possible while maintaining the validity of the constraints.

Both simulations in a virtual environment, and tests on road are made setting:

- The Lateral MPC with a prediction horizon (H_{lat}) equal to 60 steps and step width (Δ_s) of 0.5 m
- The Longitudinal MPC with a prediction horizon (H_{long}) equal to 40 steps and step width (Δ_t) of 100 ms.

The chosen prediction step is enough to represent a quasi-infinite horizon for vehicle kinematics optimization (about 30 meters or 4 seconds).

In detail, two development scenarios useful to focus on main described contents have been developed. Scenarios are defined in fig. 5.

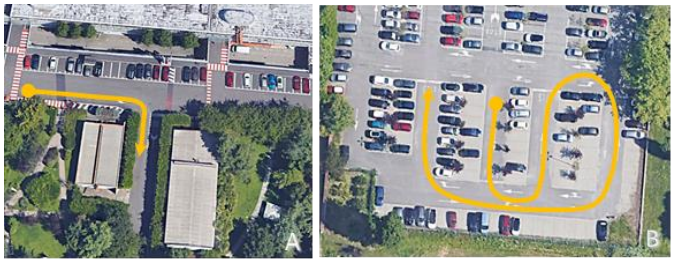

Fig. 5. *Scenarios for low speed manoeuvre used for algorithm testing in virtual environment and real proto.*

5.1 Scenario A

The first scenario foresees that the vehicle engages a curve, trying to maintain the half of the road lane and the vehicle bearing as parallel to the actual segment orientation as possible (fig. 6). The required longitudinal behavior expects to track a reference vehicle speed of 10km/h. The lateral controller is able to compute a smooth steering angle reference which satisfies the physical constraints according to (17) (fig. 8). The lateral prediction is used to realize a deceleration profile proportionate to the expected change of orientation (fig. 7) to achieve a comfortable maneuver (it can be seen from the decreasing in the speed reference at 7 sec).

Finally, it is important to underline the strategy used to stop the vehicle when it arrives at the goal. The proposed algorithm includes a longitudinal position constraint and it is demanded to the longitudinal controller to realize a comfortable stop maneuver.

Fig. 6 shows an interesting matching between developed algorithms in simulation and real-time on proto vehicle. It is possible to distinguish only limited differences between the simulation and the test on road in terms of trajectory and vehicle orientation. The same matching is also in fig. 7, mainly in the travelled distance: significant differences between reality and simulation are about vehicle speed, this is due to the fact that the implemented vehicle model is not so detailed in terms of powertrain hysteresis and non-linearities.

Also the acceleration command demonstrates differences in comparison with the simulated output of the longitudinal controller, which is again due to differences between real and simulated powertrains. In both cases, the performance in terms of comfort (speed tracking and oscillations) and distance is acceptable.

5.2 Scenario B

The second scenario is for sure most challenging and is useful to demonstrate the validity of our approach in a convincing plot. It can be considered as an automated valet parking search maneuver, with narrow spaces and two consecutive u-curves. For that maneuver the speed reference is set at 5km/h. Again the matching between simulation and real vehicle behavior is impressive in terms of trajectory and bearing (fig. 9). The differences in terms of longitudinal and lateral commands are reasonable (fig. 10, 11). This mismatch is acceptable considering a simulation tool complex enough to represent the vehicle for the model based design, and, at the same time, simple enough to be identified and maintained.

In addition to results already seen for the previous scenario (A), fig. 9 shows the rotation angle derived from (26) used to rotate the path, and fig. 13 shows the sequence of predicted trajectories at different time steps during the maneuver for scenario B. The black line is the trajectory done by the car, while the colored trends are the constraints (dashed) and the planned trajectories at each timestamp. It's very impressive to see how the planned trajectory tries to track the references and to keep the defined constraints. The sequence of plots also shows how the optimization solvers have to solve a different problem including, step by step, different path segments and different path segment orientations. This demonstrates the effectiveness of explained approach to solve a non-linear optimization problem with a linear approach based on time state control form (TSCF) transformation.

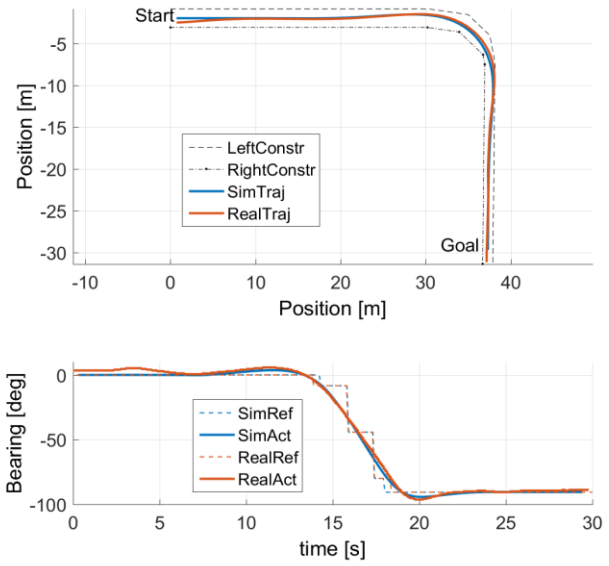

Fig. 6. *Comparison vehicle's lateral states between simulation (blue) and test on road (red)*

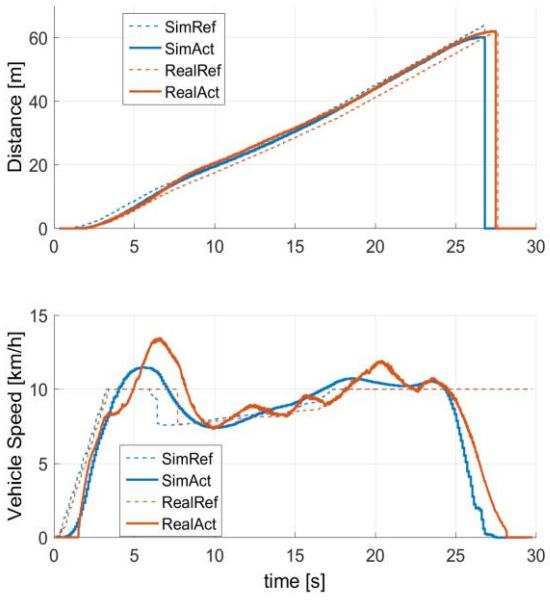

Fig. 7. *Comparison vehicle's longitudinal states between simulation (blue) and test on road (red).*

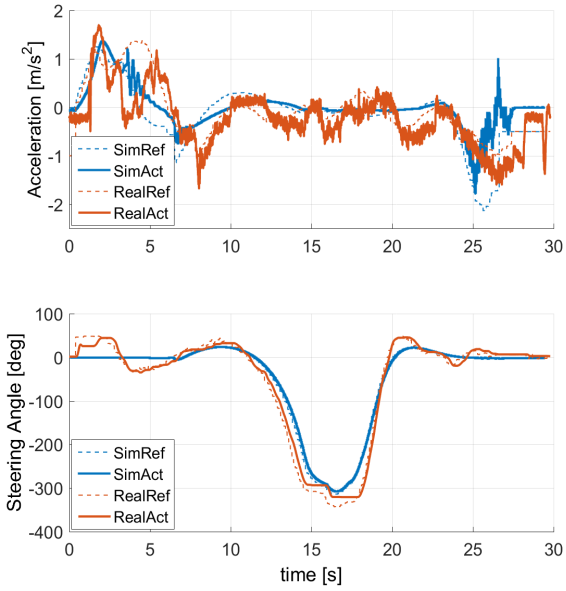

Fig. 8. *Comparison of reference and actuated Control Inputs between simulation (blue) and test on road (red).*

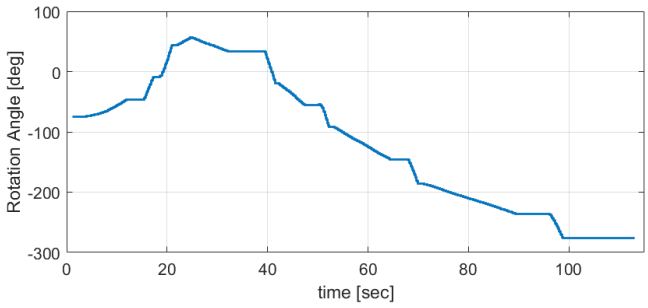

Fig. 9. *Rotation angle of MPC Reference Frame for scenario B.*

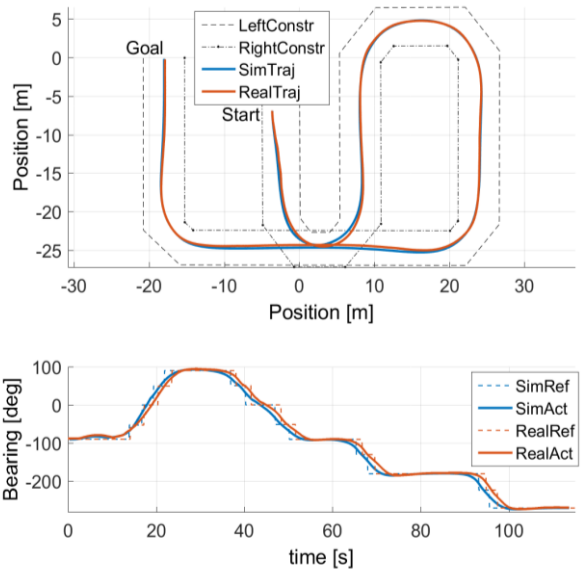

Fig. 10. *Comparison vehicle lateral states between simulation (blue) and test on road (red).*

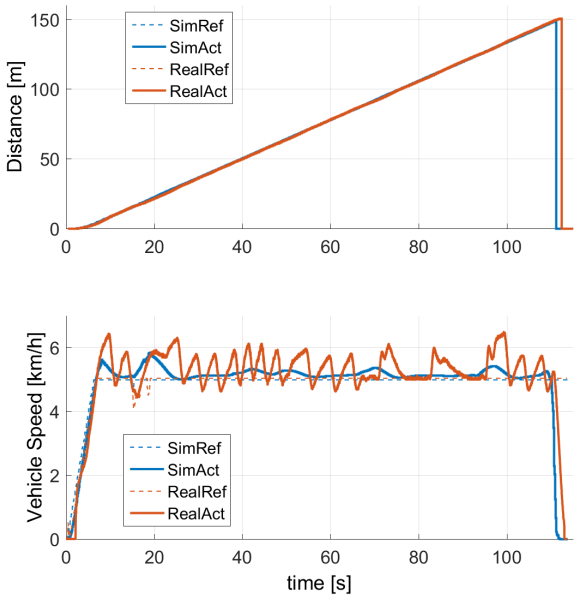

Fig. 11. *Comparison of reference and actuated Control Inputs between simulation (blue) and test on road (red).*

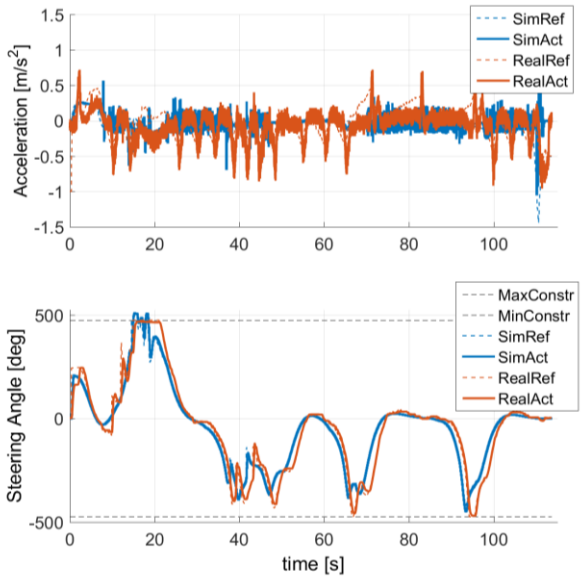

Fig. 12. *Comparison vehicle longitudinal states between simulation (blue) and test on road (red).*

6. CONCLUSIONS

This work has presented the design of a model based trajectory planning and control for vehicles at low speed. It has also shown the general approach to the problem of trajectory generation with a solution that foresees a kinematic vehicle model and guarantees the dynamical feasibility of the planned trajectory by the model-based prediction of the vehicle's motion.

This is an interesting technical solution since it does not require solving a joint optimization of longitudinal and lateral dynamics and generally lead to leads performance. The results were first evaluated in a simulation environment with IPG Car-Maker, where an initial setup has been made. From

this starting point, experimental tests have been conducted and it has have shown the performance reached by the proposed trajectory planner and controller. The car is able to properly perform a series of low speed manoeuvres defining a physically shaped trajectory.

Future work will be the extensive testing of trajectory planning in different and extended real-time scenarios in order to improve the robustness and coverage of our work. In particular, future work will refine: the constraints generation considering the vehicle size and the optimization integration with dynamic obstacles that haven't been included in the presented scenarios.

REFERENCES

US NSC Parking lot safety (2019). URL: https://www.nsc.org/road-safety/safety-topics/distracted-driving/parking-lot-safety

Trafikförsäkringsföreningen - årsredovisning 2015. URL: https://www.tff.se/globalassets/om-oss/arsredovisningar/arsredovisning-2015.pdf

Konrad Reif ed. (2015) Bosch Automotive Mechatronics, Springer Vieweg, ISBN 978-3-658-03975-2

Polack P., Altché F., D'Andréa-Novel B., De La Fortelle A. (2017). The Kinematic Bicycle Model: a Consistent Model for Planning Feasible Trajectories for Autonomous Vehicles. IEEE Intelligent Vehicles Symposium (IV), 2017.

Kong J. et al. (2015). Kinematic and dynamic vehicle models for autonomous driving control design. In: 2015 IEEE Intelligent Vehicles Symposium. 2015, pp. 1094-1099.

Oyama K. and Nonaka K. (2013). Model predictive parking control for non-holonomic vehicles using time-state control form". In 2013 European Control Conference, 458–465.

Kiyota H. and Sampei M. (1998). A control of a class of nonholonomic systems with drift using time-state control form. IFAC Nonlinear Control Systems Design, Enschede, The Netherlands, 757-762.

Raffone E. (2016). A Reduced Order Steering State Observer for Automated Steering Control Functions, in Proceedings of the 13th International Conference on Informatics in Control, Automation and Robotics, 426-432, Lisbon, Portugal.

Mattingley, J. and Boyd, S. (2012). "CVXGEN: A Code Generator for Embedded Convex Optimization". Optimization and Engineering, 12, 1-27.

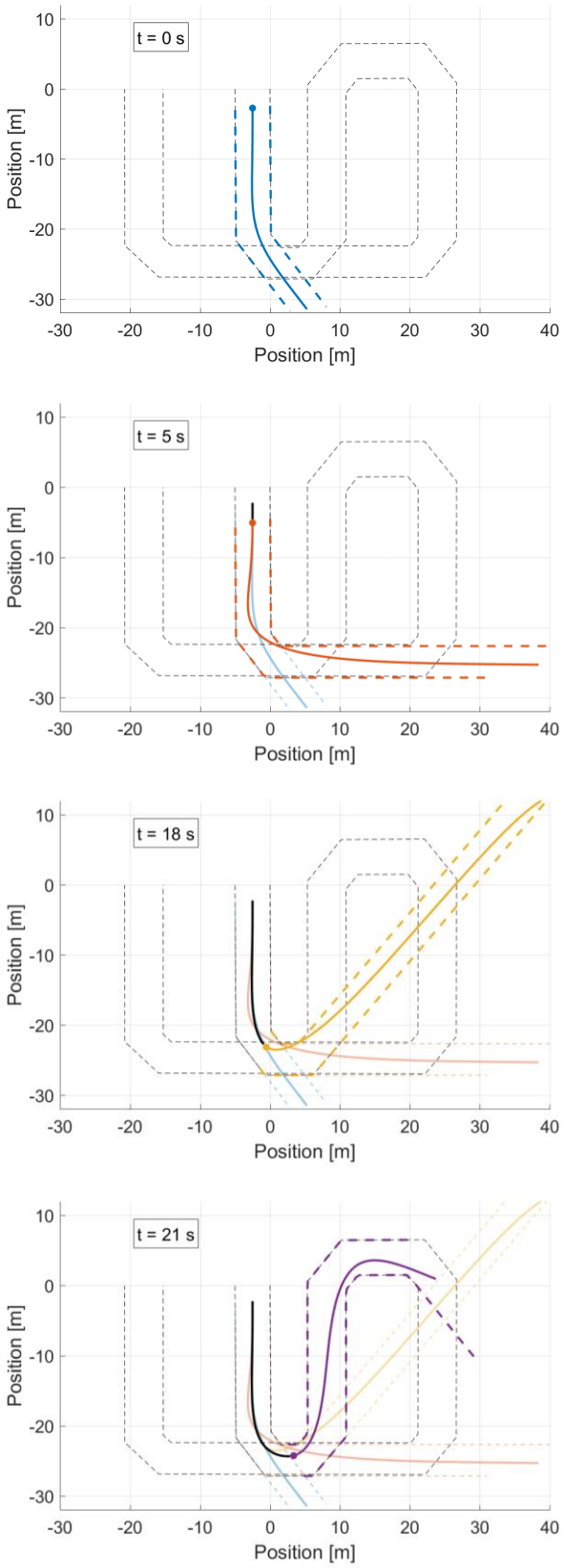

Fig. 13. *Lateral constraints and predicted trajectories by the Lateral MPC at different time stamps (coloured lines), and the travelled trajectory (black line).*